31st Congress of the International Council of the Aeronautical Sciences

Belo Horizonte, Brazil; September 09-14, 2018

DATA-DRIVEN FAILURE IDENTIFICATION USING A MOTION-BASED SIMULATOR

Aline Dahleni Kraemer*, Emilia Villani*
***Aeronautics Institute of Technology, São José dos Campos, SP, Brazil**

Keywords: *flight simulator, failure injection, failure identification, neural networks.*

Abstract

This paper presents a data-driven failure identification of flight control surfaces using neural networks. Experiments were performed in a motion-based flight simulator (SIVOR) that has been developed at Aeronautics Institute of Technology (ITA). We use a two-layer feed-forward network and we analyze the influence of the input parameters and the number of neurons in the hidden layer on the performance of the failure identification task. The evaluation of the neural network's performance is based on overall accuracy, training time, number of iterations, precision and recall. Best results were found for networks with 100 neurons in the hidden layer, presenting 97.2% of overall accuracy.

1 Introduction

A major current priority within the aircraft and aerospace community is flight safety [1,2]. Failure analysis and identification have been used to investigate events related to flight safety and aircraft accident and incident investigations throughout the years [1,3].

Actuators failures represent major threats to flight safety [4]. Physical redundancy for the actuators of the primary control surfaces is rarely available [5,6]. Furthermore, actuators failures can cause system performance deterioration or even fatal disasters if not effectively accommodated [7].

Typical Fight Control System (FCS) failure cases are runaway, jamming and oscillation of control surfaces [8], the latter is called Oscillatory Failure Case (OFC) and it will be addressed in this work.

An OFC is an abnormal oscillation of a control surface due to component malfunction in control surface servo-loops, for example, electronic components in faulty mode generating spurious harmonic signals. This oscillatory signal, of unknown amplitude and frequency, is propagated through the servo loop control, leading to control surface oscillation, and it could excite the airplane structure producing structural loads [8]. These failures may lead to unacceptably high loads or vibrations, when coupled with the aircraft aeroelastic behavior [9].

The known fault detection and identification (FDI) approaches can be classified into two categories [10]: 1) model-based and 2) data-driven schemes. The second category is currently receiving considerably increasing attention both in application and in research domains. Different from model-based approaches, in which the system's model is known a priori, the data-driven FDI methods are only dependent on the measured process variables [11].

Some solutions for the OFC are already available in the literature, mostly model-based schemes. A nonlinear actuator model is used to generate a residual on which the failure is detected by oscillation counting in [12]. The main difficulty of this approach consists in finding a systematic tuning for observation gains. Other methods are presented in [13-18].

This paper proposes a data-driven FDI approach for flight control surfaces failures using neural networks. We use a two-layer feed-forward network and we analyze the influence of the input parameters and the number of neurons in the hidden layer on the performance of the failure identification task. Flight

experiments were performed on the SIVOR simulator under normal flight conditions (without failures) and under control surfaces failure conditions (elevator and aileron failures). Data recorded from experiments were used in the data-driven FDI. The main idea is to use data frequently recorded in flight data recorders (FDRs or Black-Boxes) to perform an offline data analysis and identify flight control surfaces failures.

This paper is organized as follows: in Section 2 we present the experimental procedure. Section 3 describes the methodology used to perform failure identification. Results and discussion are presented in Section 4, followed by conclusions in Section 5.

2 Experimental procedure

This section presents the SIVOR Flight Simulator and the experiment design.

2.1 SIVOR Flight Simulator

SIVOR (*SImulador de VOo de base Robótica*, robotic flight simulator) is a project currently being developed at Aeronautics Institute of Technology (ITA) in partnership with Embraer. The goal of the project is to develop a flight simulator with a high fidelity environment and flexible so it can be reconfigured to several aircrafts of the same category. The simulation environment can be described by 4 main components: Aircraft Model, Washout Filter, Robotic Arm and Cockpit, and Pilot (Fig. 1).

i. The Aircraft Model can be configured to different types of aircraft;
ii. The Washout Filter is responsible to convert the aircraft dynamics into robot movements;
iii. The Robotic Arm and Cockpit provides a realistic flight environment for the Pilot;
iv. The Pilot closes the loop by using the inceptors (sidestick and throttle command) that provide inputs to the Aircraft Model.

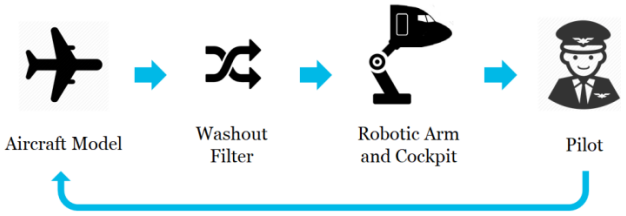

Fig. 1. Simulation Environment

The prototype of the final version of the simulator is currently in operation and it is a robotic-based flight simulator with 6 degrees of freedom (Fig. 2). This prototype was used to perform the experiments described in the next section. The aircraft model used in the experiments is a public version of the Embraer Phenom 300 and the visual system is rendered by XPlane 10™.

Fig. 2. Prototype of the SIVOR Simulator

The final version of the simulator is currently under construction and it is illustrated in Fig. 3. By installing the robotic arm into a 10 m rail, this version of the simulator has 7 degrees of freedom.

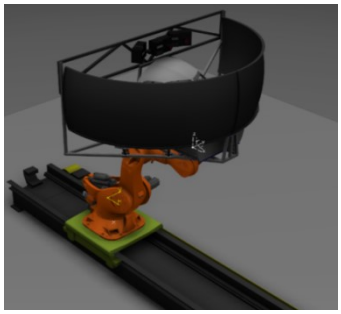

Fig. 3. SIVOR Simulator

2.2 Experiment design

The experiment was designed based on the Design of Experiments (DOE) theory proposed by Montgomery [19]. The flight path consists of a take-off maneuvre with five steps and it is presented in Fig. 4.

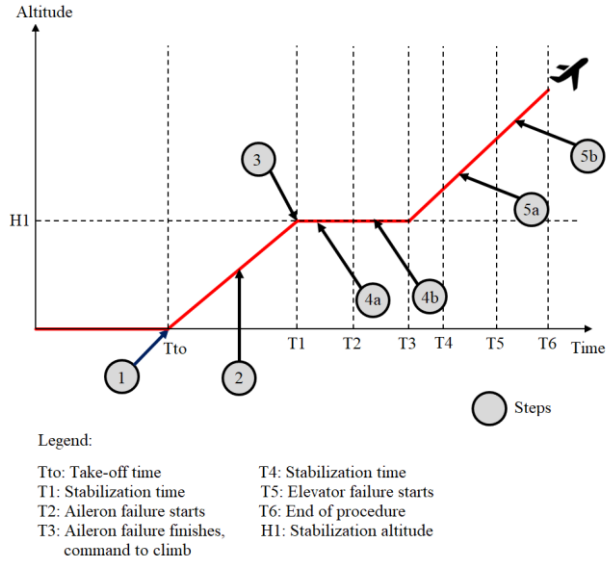

Fig. 4. Flight path

The same procedure must be followed for all flights. The initial condition is the aircraft with 100% throttle and flap 2. Then, the pilots were instructed to perform the following tasks:

i. Step 1: Execute a lift-off at 120 knots;
ii. Step 2: Maintain 140 knots until reach 3000 ft;
iii. Step 3: At 3000 ft completely retrieve flaps and landing gear, decrease the engine power to 60% and level the airplane at 3000 ft the fast as possible, executing the tasks simultaneously;
iv. Step 4a: Keep the airplane stabilized with 0° of roll;
v. Step 4b: Keep the airplane stabilized with 0° of roll with aileron failure;
vi. When instructed raise the engine power to 80% and track 15° of pitch;
vii. Step 5a: Keep the airplane stabilized with 15° of pitch;
viii. Step 5a: Keep the airplane stabilized with 15° of pitch with elevator failure.

Both aileron and elevator failures were artificially produced through an oscillatory signal applied to the correspondent control surfaces with its characteristics described by Equation 1.

$$\mathrm{N} = 0.1\sin(t) + 0.05\sin(20t) + \mathrm{random}(0.01) \quad (1)$$

where N is the signal applied to the control surface, and t is time.

The sinusoidal signal was previously adjusted according to a pilot's opinion about its intensity and controllability.

The experiment was performed by 7 pilots in two different simulation modes: with and without cabin motion. Each pilot executed 3 flights in each mode, totalizing 42 flights.

3 Methodology

This section presents the methodology that was used to develop this work.

3.1 Dataset

The analysis is based on data recorded from 41 flights. They were performed by 7 pilots, under 2 simulation modes, with 3 replicas. This configuration results in 42 experiments, but one flight was excluded due to an error in the execution of the experiment.

The recorded data was preprocessed in order to perform the data analysis considering the same start condition: the moment when the aircraft reaches 3000 ft. Furthermore, the dataset was normalized to have zero mean and unit variance (z-score normalization).

It was recorded data from the pilot commands and the aircraft behavior. In order to analyze the influence of the set of parameters on the classification accuracy, the parameters were divided into 7 different groups:

i. Group 1: pilot commands (elevator, aileron, rudder, throttle), velocity, altitude;
ii. Group 2: pilot commands (elevator, aileron, rudder, throttle), velocity, altitude, roll, pitch, heading;
iii. Group 3: pilot commands (elevator, aileron, rudder, throttle), velocity, altitude,

roll, pitch, heading, linear velocities (Vx, Vy, Vz);

iv. Group 4: pilot commands (elevator, aileron, rudder, throttle), velocity, altitude, roll, pitch, heading, Vx, Vy, Vz, angular velocities (P, Q, R);

v. Group 5: pilot commands (elevator, aileron, rudder, throttle), velocity, altitude, roll, pitch, heading, Vx, Vy, Vz, P, Q, R, engine power, engine thrust;

vi. Group 6: pilot commands (elevator, aileron, rudder, throttle), velocity, altitude, roll, pitch, heading, Vx, Vy, Vz, P, Q, R, engine power, engine thrust, control surface positions (left aileron, right aileron, elevator, rudder);

vii. Group 7: pilot commands (elevator, aileron, rudder, throttle), velocity, altitude, control surface positions (left aileron, right aileron, elevator, rudder).

3.2 Exploratory Data Analysis

Firstly we apply an initial exploratory data analysis (EDA) approach [20] to maximize insight into the dataset. We use boxplots to analyse if the classification task could be done using a simpler approach, like thresholds on specific parameters.

3.3 Neural Networks

In this work we use neural networks to solve a pattern recognition problem. The central idea of neural networks is to extract linear combinations of the inputs as derived features, and then model the target as a nonlinear function of these features. The result is a powerful learning method, with widespread applications in many fields [21].

We use a two-layer feed-forward network (Fig. 5), with sigmoid hidden and softmax output neurons, for a classification task with 3 classes: normal condition, aileron failure, and elevator failure.

The sigmoid function $\sigma(x)$, presented in Equation 2, is used as activation function in the hidden layer, with the scale parameter λ controlling the activation rate. The softmax function $g_k(T)$, presented in Equation 3, allows a final transformation of the vector of outputs T, considering a K-class classification problem.

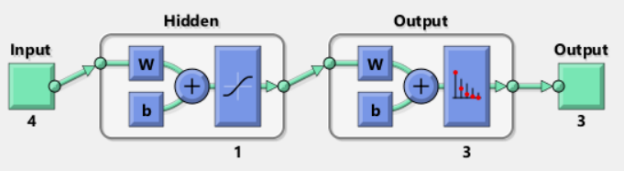

Fig. 5. Two-layer feed-forward network

$$\sigma(x) = \frac{1}{1+e^{-\lambda x}} \tag{2}$$

$$g_k(T) = \frac{e^{T_k}}{\sum_{l=1}^{K} e^{T_l}} \quad for\ k=1,\ldots,K \tag{3}$$

The number of inputs varies according to the group of parameters (Section 3.1) and the number of outputs is 3, corresponding to: normal condition, aileron failure, and elevator failure. The number of neurons in the hidden layer is varied between 1, 10, 100, 500 and 1000.

The network is trained with scaled conjugate gradient backpropagation method [22] to update weight and bias values, respectively, W and b from Fig. 5. Training automatically stops when generalization stops improving, as indicated by an increase in the cross-entropy error of the validation samples.

The dataset was divided into 3 parts: training set (50%), validation set (25%) and test set (25%) [21].

The evaluation of the neural network's performance is based on overall accuracy, training time, number of iterations, precision and recall.

The overall accuracy is the number of instances classified correctly divided by the total number of instances. Precision and recall are defined for each class, and they are calculated using the following equations [23]:

$$Precision = \frac{TP}{TP + FP} \tag{4}$$

$$Recall = \frac{TP}{TP + FN} \tag{5}$$

where TP is number of true positives, FP is the number of false positives, and FN is the number of false negatives.

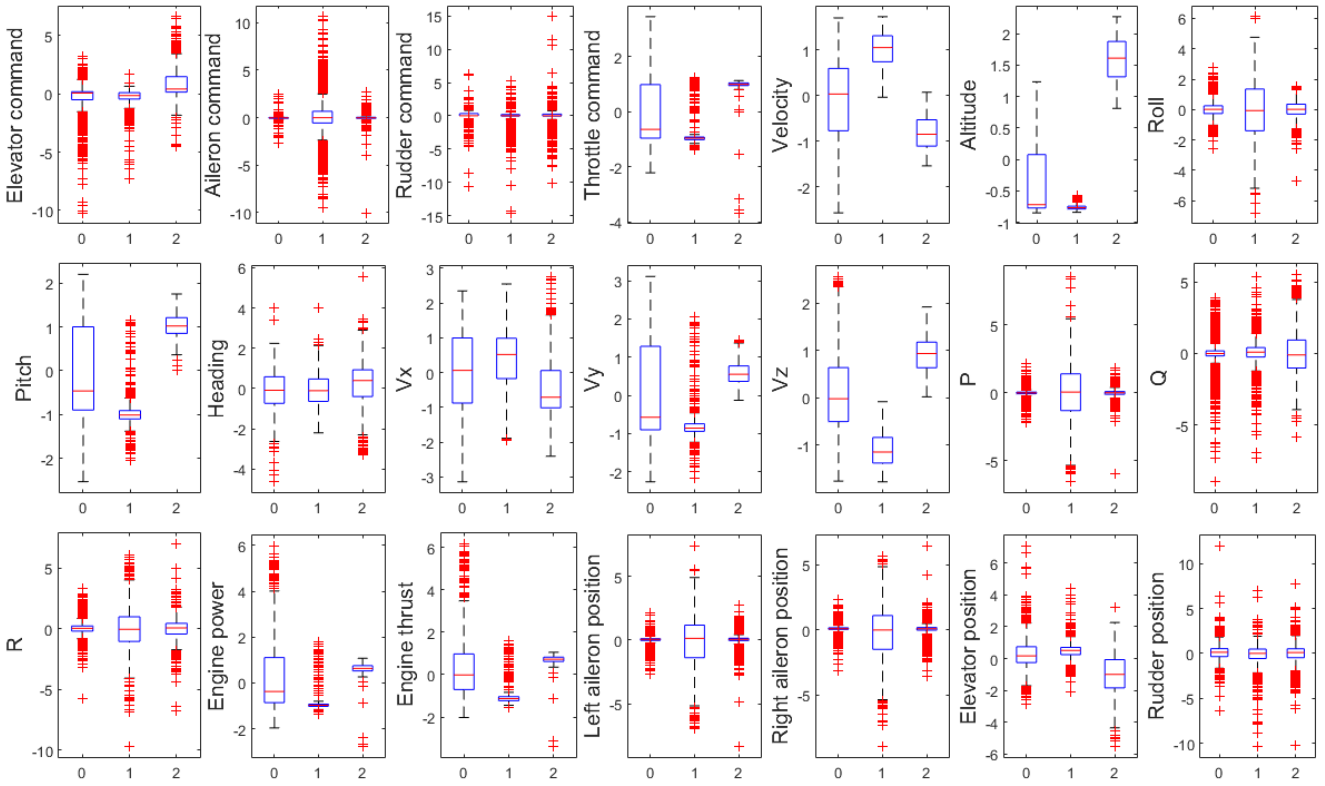

Fig. 6. Exploratory data analysis results for normal condition, aileron failure and elevator failure classes, represented by 0, 1 and 2 in the x axis, respectively.

4 Results and Discussion

This section presents the results and discussion.

4.1 Exploratory Data Analysis

Results for the exploratory data analysis are shown in Fig. 6, where the normal condition, aileron failure and elevator failure are represented by 0, 1 and 2 in the x axis, respectively. It can be seen that is not possible to distinguish between the three classes using thresholds for these parameters.

The most distinct values of median between classes are found for velocity, altitude and Vz. For altitude results, the median of the elevator failure class is higher than the other classes, mainly because of the maneuvre design, in which the elevator failure always occur in higher altitudes. However, there is still an overlap between normal and elevator failure classes. For velocity and Vz results, there is also an overlap between the classes.

4.2 Neural Networks

Results of the evaluation of neural network's performance are presented and discussed below. Results of overall accuracy are presented in Figs. 7-9, training time in Figs. 10-12, number of iterations in Figs. 13-15, and finally, precision and recall in Fig. 16.

4.2.1 Overall accuracy

The overall accuracy increases with the increase of number of neurons in the hidden layer until it reaches 100 neurons, and then it starts to decrease, as shown in Fig. 7. This behavior was expected, since at some point the increase in the number of neurons will cause overfitting. The error on the training set is driven to a very small value, but when new data (test set) is presented to the network the error is large. The network has memorized the training samples, but it has not learned to generalize to new situations.

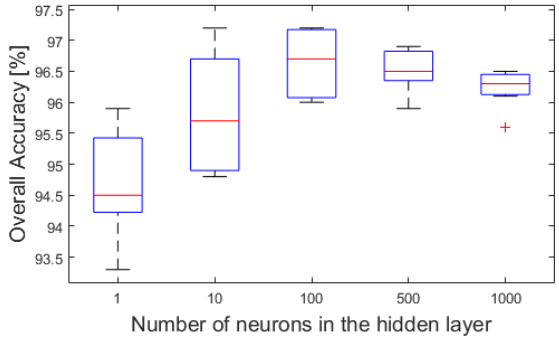

Fig. 7. Boxplot of overall accuracy, grouped by the number of neurons in the hidden layer

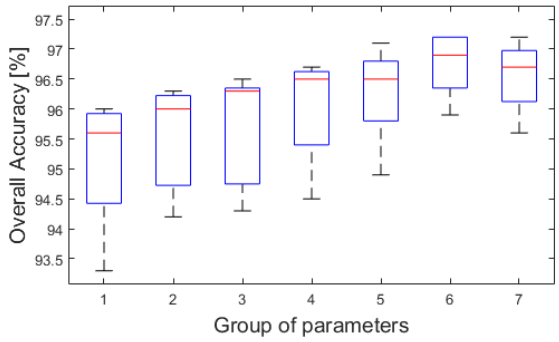

Fig. 8. Boxplot of overall accuracy for each group of parameters

The overall accuracy increases with the increase of number of parameters, as can be seen in Fig. 8. It is important to remind that from group 1 to group 6, the number of parameters increases, but the number of parameters of group 7 is smaller than group 6. This configuration was intentionally chosen to see not only the influence of the number of parameters (quantitative) but also the influence of the nature of the parameter itself (qualitative).

It can be seen in Fig. 8 that the median of the overall accuracy decreases from group 6 to group 7, the difference is 0.2%. Nevertheless, the overall accuracy for group 7 is higher than for any of the other groups between 1 and 5, even having less parameters than most of them. Group 2 has only 1 parameter less than group 7, and the median of overall accuracy is 0.7% higher for group 7. While from group 2 to 6 it is added 12 parameters and it improved the median of overall accuracy in 0.9%, from group 2 to 7 it is added only 1 parameter and it improved 0.7% the median of overall accuracy.

These results show the qualitative influence on the choice of parameters. Since the failures are related to control surfaces (aileron and elevator), using the parameters related to control surface positions improve the overall accuracy of the classification task.

The behavior of overall accuracy for different configurations of group of parameters and number of neurons in the hidden layer is presented in Fig. 9. It can be seen that the higher values for overall accuracy are found between the groups of parameters 5 and 7, and for the number of neurons in the hidden layer around 100. This summarizes the results regarding overall accuracy.

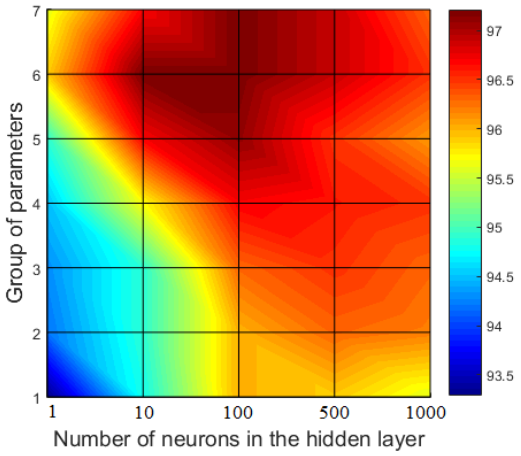

Fig. 9. Overall accuracy for different configurations of group of parameters and number of neurons in the hidden layer

4.2.2 Training time

The results for training time are shown in Figs. 10-12. From Fig. 10 it can be seen that training time increases with the increase of number of neurons in the hidden layer. The number 0 represents a training time of less than 1 second. The training time is not affected by the number of parameters, as shown in Fig. 11. These results are summarized in Fig. 12, which shows the training time for different configurations of group of parameters and number of neurons in the hidden layer.

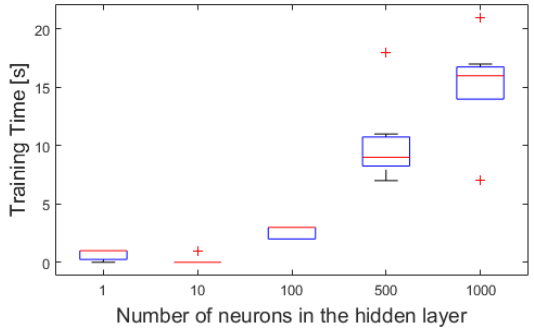

Fig. 10. Boxplot of training time, grouped by the number of neurons in the hidden layer

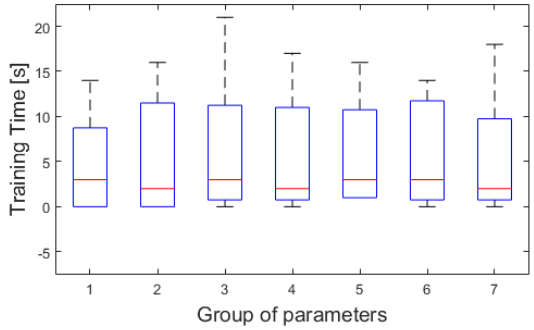

Fig. 11. Boxplot of training time for each group of parameters

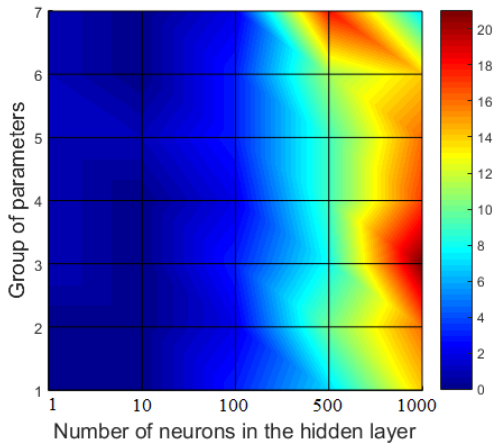

Fig. 12. Training time for different configurations of group of parameters and number of neurons in the hidden layer

4.2.3 Number of iterations

The results for the number of iterations are shown in Figs. 13-15. From Fig. 13, we noted that the highest number of iterations is found for the case with 1 neuron in the hidden layer, and for the other cases, the increase in the number of neurons has minimum effect on the number of iterations.

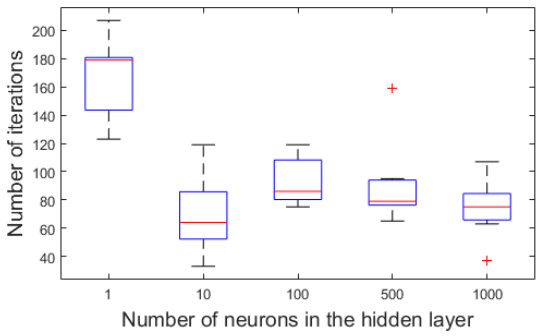

Fig. 13. Boxplot of number of iterations, grouped by the number of neurons in the hidden layer

The number of iterations does not seem to be affected by the group of parameters, as shown in Fig. 14. Figure 15 summarizes the results for number of iterations, showing its behavior for different configurations of group of parameters and number of neurons in the hidden layer.

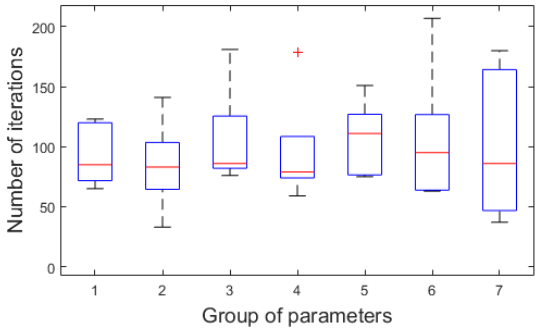

Fig. 14. Boxplot of the number of iterations for each group of parameters

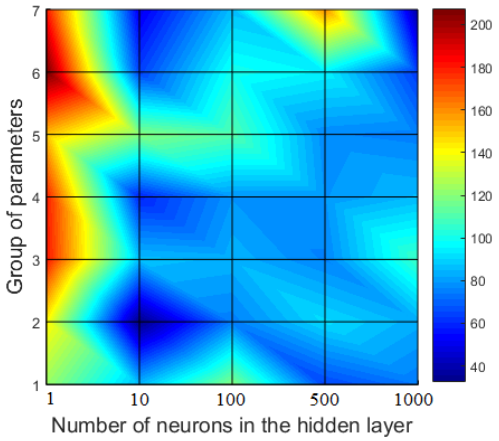

Fig. 15. Number of iterations for different configurations of group of parameters and number of neurons in the hidden layer

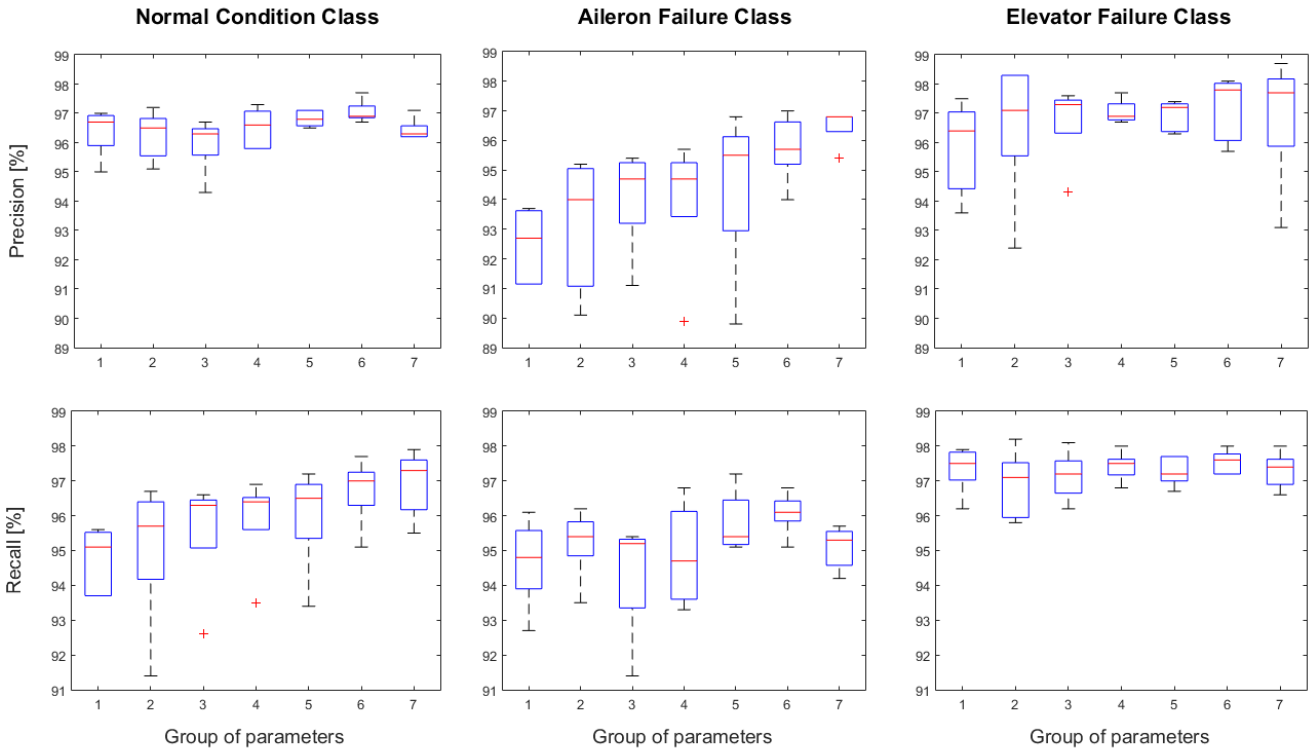

Fig. 16. Precision and recall results for each group of parameters

4.2.4 Precision and recall

Precision and recall results for each group of parameters are presented in Fig. 16. For the normal condition class, precision does not seem to be influenced by the group of parameters, while recall increases with the increase of number of parameters (from groups 1 to 6). Group 7 presents the best recall results for the normal class, even though it has less parameters.

For the aileron and elevator failure classes, recall does not seem to be affected by the group of parameters, while precision increases with the increase of the number of parameters. Group 7 presents the best precision results for the aileron failure class. The best precision results for elevator failure class are from groups 6 and 7, with similar performances.

Boxplots of precision and recall grouped by the number of neurons in the hidden layer were omitted because they present similar behavior with the overall accuracy results (Fig. 7): they increase from 1 to 100 neurons and then they start to decrease.

4.2.5 Summary of results

The overall accuracy increases with the increase of number of neurons in the hidden layer until it reaches 100 neurons, and then it starts to decrease (Fig. 7). The overall accuracy increases with the increase of number of parameters (Fig. 8). Moreover, results show the qualitative influence on the choice of parameters, since group 6 and 7 present similar values of overall accuracy, even though group 7 has less parameters than most groups.

Training time increases with the increase of number of neurons in the hidden layer (Fig. 10), and it is not affected by the group of parameters (Fig. 11).

The highest number of iterations belongs from the case with 1 neuron in the hidden layer. For the other cases, the increase in the number of neurons (Fig. 13) and parameters (Fig. 14) does not have influence on the number of iterations.

Precision increases with the increase of the number of parameters for the classes with

failure (aileron and elevator). Furthermore, recall increases with the increase of number of parameters for the normal condition class (Fig. 16).

The best results were found for 2 sets of parameters (groups 6 and 7), both cases with 100 neurons in the network hidden layer, as shown in Table 1. Considering that both presented the same overall accuracy (97.2%), and that the group 7 has less than half of group 6 number of parameters, with a smaller training time, with excellent results for recall and precision (similar with results from group 6), it can be said that the best result is achieved with group 7.

Table 1. Best results

Group of parameters	6	7
Number of parameters	21	10
Overall accuracy [%]	97.2	97.2
Training time [s]	3	2
Number of iterations	100	86
Precision for normal class [%]	96.9	97.1
Precision for aileron failure class [%]	97.0	96.6
Precision for elevator failure class [%]	98.1	98.0
Recall for normal class [%]	97.7	97.5
Recall for aileron failure class[%]	96.1	95.7
Recall for elevator failure class [%]	97.2	98.0

5 Conclusions

This paper proposed a data-driven FDI approach for flight control surfaces failures using neural networks. Flight experiments were performed on the SIVOR Simulator under normal flight conditions (without failures) and under control surfaces failure conditions (elevator and aileron failures). We used a two-layer feed-forward network and we analyzed the influence of the input parameters and the number of neurons in the hidden layer on the performance of the failure identification task. The best result was achieved by a network with 100 neurons in the hidden layer and using 10 input parameters. The overall accuracy was 97.2%, with a training time of 2 seconds, precision greater than 96.6% and recall greater than 95.7%, for all classes.

This work intends to contribute to automation of offline flight data analysis and improve flight safety.

6 Acknowledgments

This work was supported by CAPES, FAPESP (Process 2012/51085-3), FINEP/VINNOVA (Process 01.17.0038.00), CNPq (Process 303271/2017-5), Saab AB and CISB (Swedish-Brazilian Research and Innovation Center).

7 Contact Author Email Address

alinedk@ita.br

References

[1] Duarte D, Marado B, Nogueira J, Serrano B, Infante V and Moleiro F. An overview on how failure analysis contributes to flight safety in the Portuguese Air Force. *Engineering Failure Analysis*, Vol. 65, pp 86-101, July 2016.
doi: 10.1016/j.engfailanal.2016.03.003

[2] Perhinschi MG, Moncayo H, Wilburn B, Wilburn J, Karas O and Bartlett A. Neurally Augmented Immunity-Based Detection and Identification of Aircraft Sub-System Failures. *The Aeronautical Journal,* Vol. 118, No. 1205, pp. 775-796, 2014.
doi: 10.1017/S0001924000009532

[3] Zolghadri A, Le Berre H, Goupil P, Gheorghe A, Cieslak J and Dayre R. A parametric approach to fault detection in aircraft control surfaces, *AIAA Journal of Aircraft*, Vol. 53, No. 3, pp. 846–855, 2016.
doi: 10.2514/1.C032596

[4] Mack S, Tao G and Burkholder JO. Adaptive Detection of Aircraft Actuator Failures and Aerodynamic Damage. *Proc. AIAA Guidance, Navigation and Control Conference*, Toronto, Canada, August 2010.
doi: 10.2514/6.2010-8145

[5] Schram G, Gopisetty SM and Stengel RF. A fuzzy logic - parity space approach for actuator failure detection and identification. *Proc. 36th AIAA Aerospace Sciences Meeting and Exhibit*, Reno, USA, 1998.
doi: 10.2514/6.1998-1014

[6] Perhinschi MG, Napolitano MR, Campa G and Fravolini ML. Primary control surface failure detection and identification scheme. *Proc. AIAA Guidance Navigation Control Conf.*, Austin, USA, 2003.

doi: 10.2514/6.2003-5645

[7] Liu Y and Tao G. Model-based direct adaptive actuator failure compensation techniques with applications to aircraft flight control systems. *Proc. of AIAA Guidance, Navigation, and Control Conference*, AIAA-2006-6554, 2006.

[8] Efimov D, Cieslak J, Zolghadri A and Henry D. Actuator fault detection in aircraft systems: Oscillatory failure case study. *Annual Reviews in Control*, Vol. 37, No. 1, pp 180-190, 2013. doi:10.1016/j.arcontrol.2013.04.007

[9] Goupil P. AIRBUS state of the art and practices on FDI and FTC in flight control system. *Control Engineering Practice,* Vol. 19, No. 6, pp 524-539, 2011. doi:10.1016/j.conengprac.2010.12.009

[10] Zhang YM and Jiang J. Bibliographical Review on Reconfigurable Fault-Tolerant Control Systems. *Annual Reviews in Control*, Vol. 32, No. 2, pp. 229-252, 2008. doi: 10.1016/j.arcontrol.2008.03.008

[11] Yin S, Ding SX, Haghani A, Hao H and Zhang P. A comparison study of basic data-driven fault diagnosis and process monitoring methods on the benchmark Tennessee Eastman process. *Journal of Process Control*, Vol. 22, No.9, pp 1567-1581, 2012. doi: 10.1016/j.jprocont.2012.06.009

[12] Goupil P. Oscillatory failure case detection in the A380 electrical flight control system by analytical redundancy. *Control Engineering Practice,* Vol. 18, No. 9, pp 1110-1119, 2010. doi: 10.1016/j.conengprac.2009.04.003

[13] Alwi H and Edwards C. Oscillatory Failure Case Detection For Aircraft Using an Adaptive Sliding Mode Differentiator Scheme. *Proceedings of the 2011 American Control Conference*, San Francisco, pp 1384-1389, 2011. doi: 10.1109/ACC.2011.5991247

[14] Alwi H and Edwards C. An adaptive sliding mode differentiator for actuator oscillatory failure case reconstruction. *Automatica,* Vol. 49, No. 2, pp 642 - 651, 2013. doi: 10.1016/j.automatica.2012.11.042

[15] Pons R, Jauberthie C, Trav-Massuys L and Goupil P. Control surfaces oscillatory failures identification using interval analysis. *Proceedings of the 19th International Workshop on Principles of Diagnosis (DX-08)*, Blue Mountains, Australia, 2008.

[16] Lavigne L, Zolghadri A, Goupil P and Simon P. Robust and early detection of oscillatory failure case for new generation AIRBUS aircraft. *Proceedings of the AIAA Guidance, Navigation and Control Conference and Exhibit*, Honolulu, Hawaii, 2008. doi: 10.2514/6.2008-7139

[17] Alcorta-Garcia E, Zolghadri A, and Goupil P. A nonlinear observer-based strategy for aircraft oscillatory failure detection: A380 case study. *IEEE Transactions on Aerospace and Electronic Systems*, Vol. 47, No. 4, pp 2792–2806, 2011.

[18] Sachs H, Gojny MH and Carl UB. Robust detection of oscillatory and transient aircraft actuation system failures using analytical redundancy. Proceedings of the SAE 2009 AeroTech Congress & Exhibition, Seattle, 2009.

[19] Montgomery DC. *Design and Analysis of Experiments*. 8th edition, John Wiley & Sons, 2013. doi: 10.1198/tech.2006.s372

[20] Tukey JW. *Exploratory Data Analysis*, Pearson, 1977.

[21] Hastie T, Tibshirani R and Friedman J. *The elements of Statistical Learning: Data Mining, Inference, and Prediction*. 2nd edition, Springer, 2008.

[22] Møller MF. A scaled conjugate gradient algorithm for fast supervised learning. *Neural Networks*, Vol. 6, No. 4, pp 525-533, 1993. doi: 10.1016/S0893-6080(05)80056-5

[23] Raschka, S. *Python Machine Learning*. Packt Publishing, 2015.

Copyright Statement